12

Numerical Simulation Techniques for the Prediction of Fluid-Dynamics, Combustion and Performance in IC Engines Fuelled by CNG

Mirko Baratta and Ezio Spessa
IC Engines Advanced Laboratory – Politecnico di Torino, Torino
Italy

1. Introduction

The design of modern internal combustion (IC) engines requires the understanding and quantification of many physical phenomena, including their impact on engine performance and emissions. In fact, the investigation of thermo-fluid-dynamic processes, combustion, performance and emissions is essential to fulfil the emission regulations, that are becoming more and more severe. Although the experimental analysis of such processes is mandatory to obtain fully quantitative results, the application of numerical simulation techniques is continuously increasing in popularity amongst the research community. This is due, on one hand, to the increased accuracy of specific sub-models, which are dedicated to several physical aspects in IC engines, and, on the other hand, to the availability of computational resources of increasing power. Nowadays, simulation tools can range from zero-dimensional analysis tools of the combustion process in the engine chamber, to complete three-dimensional simulation models of turbulent flows and combustion.
This chapter is intended as an overview of the state-of-the-art of 1-D computational fluid-dynamics (CFD) and thermo-dynamic tools applied to IC engines, with specific reference to compressed natural gas (CNG) fuelling. Moreover, the specific modelling approaches of the authors are presented, within the 0-D and 1-D frameworks.

2. 1-D engine simulation

1-D simulation tools are based on the solution of the inviscid form of the conservation laws of mass, momentum and energy (Euler equations). The equations are actually written in a 'generalized' form, in which ad-hoc terms are added, in order to properly simulate the friction and heat-exchange effects at the pipe walls. Furthermore, they are written in a quasi 1-D approach, as the variations of any dependent variable in a direction orthogonal to the flow direction are neglected, and at the same time the changes in the flow cross-section along the pipe axis are accounted for.
In the last two decades, several commercial 1-D CFD tools have specifically been developed for engine flow simulation: among others, GT-Power (Gamma Technologies), Wave (Ricardo), Boost (AVL), and AMESim (LSM). Among the different classes of computational models, such tools are often a good compromise between accuracy, the required CPU time, and completeness of the engine system that can be analyzed.

1-D codes are designed to simulate the unsteady flow throughout the whole engine system, as well as throughout the whole engine cycle. The essential processes of the complete engine system are described by means of mathematical equations in such a way that the physical states, such as pressures, temperatures and mass flows, can be calculated in all the computational volumes and at all the instants. These codes allow the calculation of any engine-relevant cycle-averaged parameter which is useful for the assessment of the engine performance: torque, power, indicated work, volumetric efficiency, fuel consumption, and so on. Engine-oriented 1-D codes have increasingly been used in order to support the engine design phase (Winterbone & Pearson, 1990; Blair, 1999). Their application usually starts from the calibration of an engine model in a 'baseline' configuration, on the basis of experimental data. Then, the predictive model is used to estimate the impact of a different engine configuration on the performance, the efficiency and the emission levels: among others, the inlet and exhaust pipes length and diameter, the turbocharger characteristics, the valve actuation and timing, and the combustion-management strategies, can be modified (Badami et al., 2002; Baratta et al., 2010; Galindo et al., 2004; Vitek et al., 2006). 1-D codes are often used to provide time-dependent boundary conditions for three-dimensional in-cylinder turbulent-flow simulations.

The quasi 1-D approach is adopted in the engine intake and exhaust systems, which can be considered as assemblies of pipe elements. Other engine components are modelled by means of the zero-dimensional approach, usually combined with ad-hoc lumped parameter models or performance maps. Cylinders, injectors, valves, compressors and turbines are simulated in this way, and their behaviour is properly coupled to that of the 1-D computational domain.

A brief overview of the main engine-components modelling approaches is provided hereafter. Then, the main issues concerning the model tuning procedure are discussed.

2.1 Cylinders

For the mathematical description of the physical processes that occur within cylinders, it is worth distinguishing between the gas exchange and the high-pressure phase. Only during the gas exchange, do mass flows occur between the cylinder and the connected pipes and manifolds through the valves. Cylinders are usually zero-dimensional parts in which a uniform pressure is assumed. The temperature is considered uniform in the gas exchange phase and in the high-pressure cycle prior to the start of combustion, whereas a two-zone (burned-unburned) methodology is followed after the start of combustion and prior to the opening of the exhaust valve (see, for example, Gamma Technologies, 2009). Sometimes a multizone approach is followed, in order to accurately describe the burned-gas temperature distribution and the pollutant formation mechanisms (Baratta et al., 2006, 2008; Onorati et al., 2003).

When one or more valves are open, the cylinder-content evolution is governed by the continuity equation and the First Law of Thermodynamics:

$$dm_{cyl} = \left(\dot{m}_{in} - \dot{m}_{out}\right) dt \tag{1}$$

$$-dQ + pdV_{cyl} = d\left(m_{cyl}U_{cyl}\right) + \left(\dot{m}_{out}i_{cyl} - \dot{m}_{in}i_{in}\right) dt \tag{2}$$

in which the symbols U and i denote the internal energy and the enthalpy, respectively, Q is the heat transfer to the walls, and V_{cyl} is the instantaneous chamber volume. During the

high-pressure phase, flow leakages from the combustion chamber are usually neglected, which means that the trapped-air mass m_{cyl} is considered constant. The charge thermodynamic state can be calculated, prior to the start of combustion, by solving the First Law of Thermodynamics, under the assumption of a constant mass and considering a uniform temperature distribution inside the chamber (single-zone approach):

$$-dQ + pdV_{cyl} = m_{cyl}dU_{cyl} \tag{3}$$

It should be noted that a suitable correlation for the heat transfer between the charge and the cylinder walls is needed (Catania et al., 2001; Heywood, 1988): this point will be discussed in the following subsection.

After the onset of combustion, four variables are required, whenever the two-zone approach is followed, to define the charge state, at each time step: pressure (p), unburned and burned-gas temperature (T_u and T_b, respectively), and burned-mass fraction ($x_b = \frac{m_b}{m_{tot}} = \frac{m_b}{m_b + m_u}$).

Although the exact set of equations which is actually implemented can be different from one distributed code to another, a general framework exists. The required variables are calculated by implementing a suitable form of the energy conservation equation for the unburned zone and for the whole cylinder content, of the conservation of the instantaneous cylinder volume, and of a so-called 'combustion model'.

The formulation of the energy conservation law is common to both simulation and diagnostic models, and can be written in the following form (Catania et al., 2003):

Unburned-gas region:

$$-dQ_u + V_u dp = \left(1 - x_b\right) m_{cyl}\, di_u \tag{4}$$

Cylinder content:

$$-\left(dQ_u + dQ_b\right) + V_{cyl}dp = \left(i_b - i_u\right) m_{cyl}\, dx_b + \left(1 - x_b\right) m_{cyl}\, di_u + m_{cyl}\, x_b\, di_b \tag{5}$$

The conservation of the chamber volume can be used to derive an equation that links the pressure at a given crank angle to T_u, T_b, and x_b (Baratta et al., 2006):

$$\mathrm{p} = \frac{m_{cyl}}{V_{cyl}}\left[\left(1 - x_b\right) R_u T_u + x_b R_b T_b\right] \tag{6}$$

The enthalpy of the burned and unburned gases is determined in Eqs. (4-5) for each chemical species, by means of polynomial functions of the gas temperature. JANAF tables can be used for this purpose (Baratta et al., 2006; Catania et al., 2003, 2004). The unburned-gas enthalpy includes the contribution of the fuel chemical energy which is released during combustion. The equation set is closed by introducing a 'combustion model', that allows x_b in Eqs. (4-6) to be defined. Combustion modelling is a fundamental feature of engine simulation codes. Its primary objective is to predict, or to specify, the rate of heat release (that is, the rate at which the chemical energy of a fuel is converted into thermal energy of burned gases) and hence the in-cylinder pressure evolution. Basically, the combustion model can be non-predictive or predictive.

A non-predictive combustion model simply imposes a burn rate as a function of the crank angle. The prescribed burn rate will be followed, regardless of the conditions inside the

cylinder. With reference to SI engines, the Wiebe function allows the almost S-shape of experimentally observed burn rates to be reproduced (Heywood, 1988). The Wiebe function is completely straightforward to apply, but on the other hand, it does not contain any description of the various physical phenomena, such as the in-cylinder turbulence level or flame-turbulence interaction. Hence, such an approach should only be followed when the purpose of the engine simulation model is to investigate the effect of a variable that virtually does not influence the burn rate. The accuracy of the Wiebe-function approach can be enhanced by including ad-hoc lookup tables in the model for the Wiebe parameters. This procedure has successfully been followed by many researchers (see, for example, Baratta et al., 2010; Lefebvre & Guilain, 2005). In (Baratta et al., 2010), a large number of experiments were carried out on an engine test rig under steady-state operating conditions at different engine speed (N) and brake mean effective pressure (bmep) values. A heat-release analysis was then carried out with the specific tools embedded in GT-Power, and the obtained parameters were organized in lookup tables as functions of N and bmep.
An alternative approach, which was pioneered in (Blizzard & Keck, 1974), is to use predictive combustion models. These models consist of phenomenological correlations for the turbulent burning speed, and are based on physical principles, so that they can account for any changes in the in-cylinder flow, combustion chamber geometry, mixture properties and thermodynamic state, spark timing, and so on. The topic of predictive combustion models will be dealth with in a dedicated section of this chapter.

2.2 In-cylinder heat transfer

In a zero-dimensional first-law analysis of the indicated cycle in an IC engine (Eqs. 1-6), the heat transfer term has to be estimated. This is usually done on an instantaneous, spatially average basis, using Newton's law:

$$\frac{dQ}{dt} = h \cdot A \cdot \left(T - T_w\right) \tag{7}$$

where h is the convective heat-transfer coefficient, A is the gas-wall contact area, T is the gas temperature, T_w is the wall temperature. The Woschni correlation (Sihling & Woschni, 1979; Woschni, 1967) is by far the most frequently applied relation for this purpose. The Woschni correlation defines a spatially-averaged convective coefficient:

$$h\left[\frac{W}{m^2 K}\right] = c_0 \cdot D[m]^{-0.2}\, p[bar]^{0.8}\, T[K]^{-0.55}\, w\left[\frac{m}{s}\right]^{0.8} \tag{8}$$

where, in the original Woschni's paper, c_0=130, and w is an average gas velocity, which was assumed to be made up of a term proportional to the mean piston speed, and another proportional to the difference between the instantaneous pressure and the instantaneous motored pressure (at the same crank angle).
As far as the c_0 coefficient is concerned, there is evidence in the literature that a fine tuning is needed if accurate results are desired (Baratta et al., 2005; Catania et al., 2003; Guezennec & Hamada, 1999). Tuning can be performed when the Woschni correlation is applied to estimate the heat transfer in a diagnostic tool, in which the experimental in-cylinder pressure trace is analyzed and the heat-release law is calculated. For example, a method for calibrating the heat transfer coefficient was proposed and assessed in (Catania et al., 2003), based on the measurement of the exhaust emissions, with specific reference to HC, CO, and

H_2, and on an energy balance of the whole cylinder charge, from the start to the end of combustion. When the correlation is employed for predictive indicated-cycle calculations, the heat transfer coefficient can be set on the basis of experience previously acquired on similar engines, or can be calibrated at a few engine working points with the support of experimental tests, combined with diagnostic analysis. Lookup tables for c_0 can then be included in the engine model.

A different approach can be followed if a predictive combustion model is applied, as will be detailed in the 'Predictive 0-D combustion models' section of this chapter. Since such a combustion model needs the support of a zero-dimensional in-cylinder fluid flow and turbulence submodels, the same flow model is sometimes used to estimate an equivalent fluid velocity and, hence, the convective heat transfer coefficient (see, for example, Gamma Technologies, 2009; Hountalas & Pariotis, 2001; Morel & Keribar, 1985).

Although most of engine 1-D simulation codes determine the instantaneous heat flux through Eq. (7), many research works (Alkidas, 1980; Catania et al., 2001; Enomoto & Furuhama, 1989) have pointed out a phase lag and an attenuation of the heat flux calculated using the conventional convection law, with respect to the measured heat-flux distributions vs. crank angle. For this reason, in order to take the unsteadiness of the gas-wall temperature difference into account, the following unsteady formulation for Newton's convection law was proposed in (Catania et al., 2001):

$$Q = h \cdot A \cdot \left[T - T_w + K \frac{B}{S_p} \frac{d\left(T - T_w\right)}{dt} \right] \qquad (9)$$

where: B is the bore diameter, S_p the mean piston speed, and K a dimensionless coefficient that has to be calibrated.

2.3 Turbochargers

The turbocharger sub-model is a critical part of the overall model of a turbocharged engine. The approach followed in most 1-D simulation tools is to include turbocharger performance data in the form of lookup tables (Gamma Technologies, 2009), which are processed by the software in order to obtain the final interpolated maps. The interpolation procedure can be either fully automatic or partially controlled by the user. However, the final map quality is dependent to a great extent on the amount and quality of the available experimental data, which are usually measured in a flow rig under steady-state conditions.

The detailed turbocharger modelling technique which is followed by the GT-Power code is described hereafter. The approach is similar to those followed by the other codes that are available in the market.

GT-Power handles measured compressor and turbine performance tables in SAE format, in which the data are organized as several "speed lines" according to standards J922 and J1826. The data for each speed line consist of mass flow rate, pressure ratio and thermodynamic efficiency triplets. As an example, Fig. 1 shows the raw turbine map data for a turbocharger which is installed on a 7.8 litre CNG engine (Baratta et al., 2010), in terms of reduced mass flow (graph on the left) and efficiency (graph on the right) versus pressure ratio for different speed lines. Quantities on abscissa and vertical axis have been normalized to their maximum value. Each coloured line refers to a different reduced speed n_{red}. In GT-Power, the performance tables are pre-processed so as to create internal maps that define the

performance of the turbine and compressor over a wide range of operating conditions. The topic of turbine table pre-processing is described hereafter, as it is generally accepted that turbine data quality is the most critical point in turbocharged engine simulation (Baratta et al., 2010; Westin & Ångström, 2003; Westin et al., 2004; Winkler & Ångström, 2007). Turbine data pre-processing uses the well-known characteristics of turbines regarding efficiency, reduced mass flow rates and blade speed ratio (BSR). Namely, for a fixed-geometry turbine, the efficiency and reduced mass flow rate should lie on specific trend lines when plotted against $BSR = U/C_S$, provided each quantity is normalized to its value at the maximum efficiency point on the actual speed line. U is the rotor blade tip speed and C_S is the gas velocity that would be achieved by an isentropic expansion across the turbine stage. The application of the GT-Power approach to the turbocharger data in Fig. 1 is shown in Fig. 2a,b. The agreement between the experimental data and the fit curves in Fig. 2a,b highlights the accuracy of the procedure for a wide range of BSR values. Figures 2c,d show the complete extent of the mass flow and efficiency maps, which are obtained on the basis of the fit curves, including the extrapolated ranges of n_{red} and PR. These plots are a graphical representation of the maps used internally by the code for the turbocharger simulation.

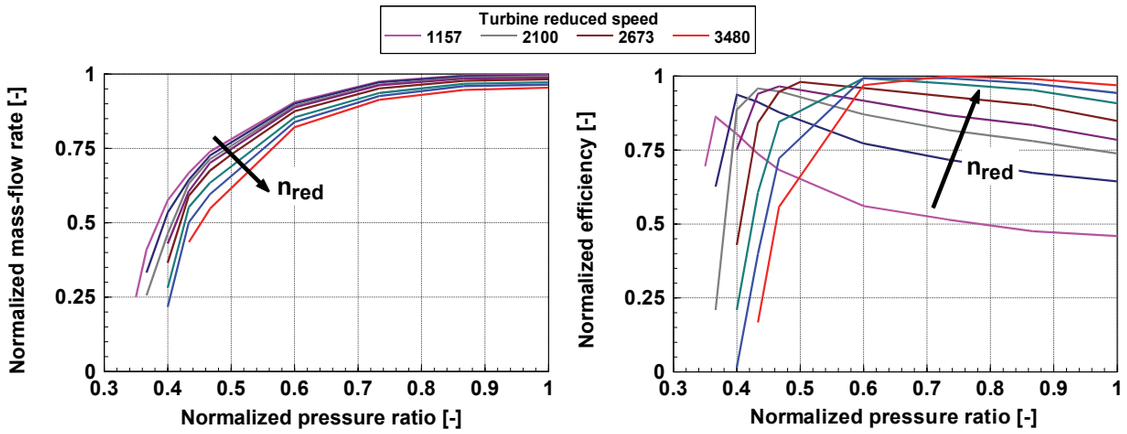

Fig. 1. Raw turbine performance maps. Each quantity is normalized to a specific value (Baratta et al., 2010).

The turbocharger maps are lumped-parameter models which are fluid-dynamically coupled to the surrounding 1-D pipe elements. For a given pressure ratio (imposed by the pipes at the compressor and turbine boundaries), and for a given shaft speed, which is the same for both the compressor and the turbine, the maps provide a value of the mass-flow rate and the efficiency. Such values can be adjusted by means of a mass-flow and an efficiency multiplier (MFM and EM, respectively), and are then used in the calculations. The mass-flow rate is imposed as a boundary condition in the adjacent pipes, and the PR and the efficiency are used to compute the instantaneous turbine and compressor power. The unbalance between these powers determines the change in the shaft speed in the actual time step, according to the following equation:

$$\frac{1}{\omega_{shaft}}\left(\dot{m}_{exh}\eta_{trb}c_p{}'T^0_{in,trb}\cdot\left(1-PR^{1-\gamma'/\gamma'}\right)-\dot{m}_{air}\frac{1}{\eta_{cmp}}c_pT^0_{in,cmp}\left(PR_{cmp}^{\gamma-1/\gamma}-1\right)\right)=I_{TC}\frac{d\omega_{shaft}}{dt} \quad (10)$$

where $\dot{m}_{air}$ is the mass flow rate through the compressor, $\dot{m}_{exh}$ is the mass flow rate of the exhaust gases through the turbine, c_p is the specific heat at a constant pressure of the air, γ is the ratio of the specific heats of the air, γ' is the ratio of the specific heats of the exhaust gases, $T^0_{in,cmp}$ is the total gas temperature at the compressor inlet, PR_{cmp} is the pressure ratio across the compressor, and η_{cmp} and η_{trb} are the efficiencies of the compressor and the turbine, respectively. Finally, ω_{shaft} is the shaft rotational speed, and I_{TC} denotes the whole turbocharger (compressor, turbine and shaft) inertia.

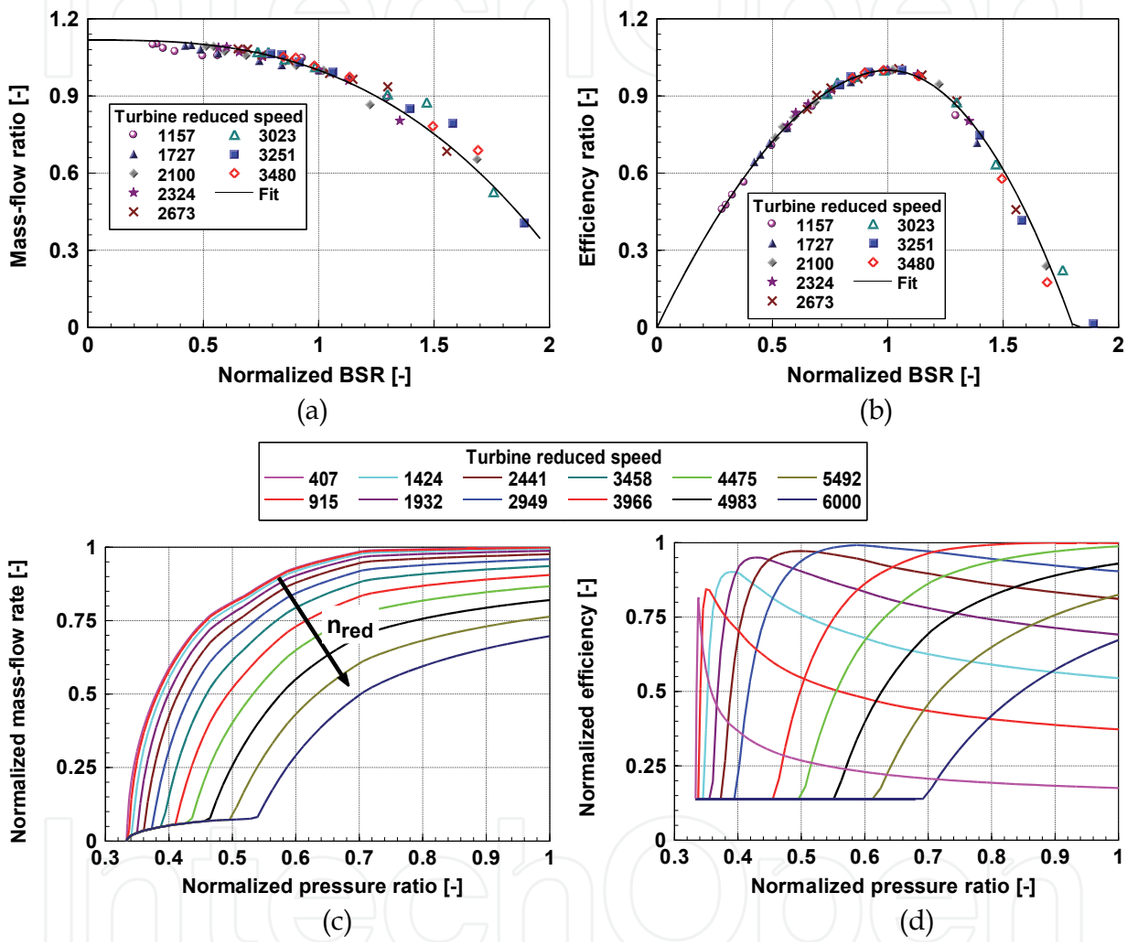

Fig. 2. Turbine performance maps. (a), (b) mass flow and efficiency fit versus data as functions of BSR; (c), (d) final turbine mass flow and efficiency maps, including the extrapolated range of reduced speed and PR (Baratta et al., 2010).

2.4 Performance of compressors and turbines

The potential need to adjust the mass-flow or the efficiency multipliers has long been known (Baratta et al., 2010; Gamma Technologies, 2009; Westin & Ångström, 2003; Westin et al., 2004).

As far as the compressor is concerned, differences in installation may influence the compressor surge-line shape, as surge depends on the compressor inlet and delivery arrangements (Baines, 2005). The position of the surge line will therefore vary from the gas

stand to the engine, and from one engine installation to another. Fortunately, these variations are quite small in many cases. Due to the limited extent of the pulsating flow, which is usually observed at the compressor side, it has been found that the compressor averaging point can be predicted with good accuracy without having to adjust the compressor map. Both the compressor speed and pressure ratio usually fit well the measured values (Westin & Ångström, 2003).

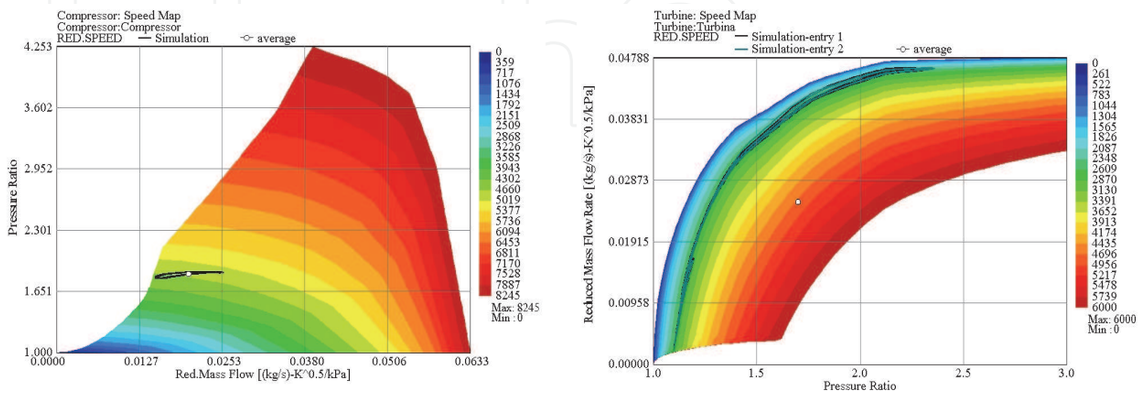

Fig. 3. Simulated compressor and turbine operating points for the maximum torque operation point of a TC 7.8 litre CNG engine. Steady-state engine operating conditions, $N = 0.55\ N_{max}$.

Conversely, the power from the turbine often has to be adjusted for each single operating conditions for many reasons (Westin et al., 2004):

- The flow entering the turbine in the engine installation is heavily pulsating, whereas the turbine performance maps are usually measured under steady-state conditions;
- During each engine cycle, the pulsating flow covers a large operating range, and this means that a large portion of the map is covered for each cycle. Often, the map is not measured with a large enough range, thus the software needs to extrapolate it, and this extrapolation may be a source of error;
- In most cases, the maps are not measured for the low-speed range of the turbocharger. Consequently, for low engine speeds, the calculation depends on a map portion which is usually extrapolated;
- The engine exhaust temperatures can be substantially higher than the gas temperatures used when measuring the maps.

Figure 3 shows the simulated compressor and turbine operating points for the maximum torque operation point of a TC 7.8 litre CNG engine (Baratta et al., 2010), under steady-state engine operating conditions. The black lines show the excursion of the compressor and turbine working point on the map during the engine cycle (two lines are plotted for the turbine, which is of the twin-entry type). The empty circles denote 'average' points, which are given by the time-average of the mass-flow rate and pressure ratio. The different extent of the pulsating flow at the compressor and at the turbine side is apparent.

As regards the turbine, the EM factor actually accounts for two processes (Baines, 2005): the fraction of the exhaust-gas energy that is available at the turbine inlet, which depends on the engine exhaust-pipes arrangements, and the efficiency with which the turbine converts this energy into shaft work. The correction does not, therefore, necessarily mean higher or lower

turbine efficiency under pulse-flow conditions, but rather that the overall efficiency of the whole exhaust system is different. This has recently been referred to as 'apparent pulse turbine efficiency' (Baines, 2005; Watson & Janota, 1982).
The necessity of adjusting the turbine efficiency for each operation point would mean that is practically impossible to build a fully predictive 1-D model for a turbocharged engine. However, the problem can be overcome by organizing the turbine efficiency multipliers, obtained in the calibrated points, in a suitable form. For example, in (Baratta et al., 2010), the calibration of the turbine efficiency was carried out over a wide range of engine speeds and loads, with reference to a Heavy-Duty turbocharged CNG engine, and the obtained efficiency multiplier resulted to have a well defined trend when plotted against the turbine expansion ratio, as shown in Fig. 4. Such a trend is in agreement with the findings of (Watson & Janota, 1982), as well as with those of (Westin & Ångström, 2003), who calculated a multiplier value of 1.42 at partial load (i.e., low turbine expansion ratio) and of 0.69 at full load, for a 4-cylinder 2 litre gasoline-fuelled SI engine. $\eta_{trb,apparent}$ in Fig. 4 corresponds to η_{trb} in Eq. (10).

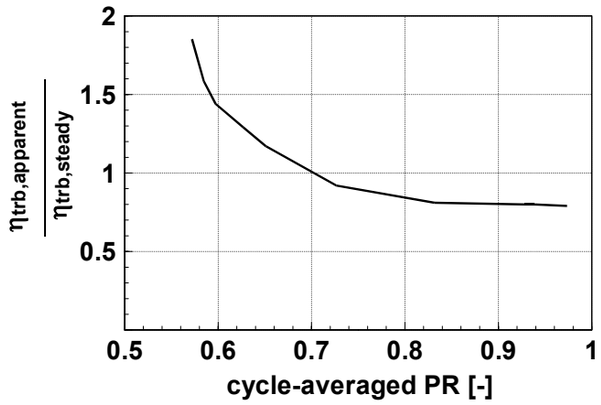

Fig. 4. Ratio of apparent turbine efficiency under pulsating flow conditions to steady-state flow efficiency. Cycle-averaged PR is normalized to a specific value (Baratta et al., 2010).

The turbine efficiency multiplier data, organized as in Fig. 4, can be very useful to allow the model to make reliable predictions of the turbine behaviour outside the calibration points. Furthermore, they are even more important if a transient simulation has to be performed. For example, (Baratta et al., 2010) considered the simulation of engine load transients at fixed speed, and almost the whole curve reported in Fig. 4 was used by the software during the calculations.
Finally, it is worth stressing that heat losses from the turbine are usually neglected in the simulations. (Westin et al., 2004) proposed an approach, based on experimental heat-transfer measurements, to account for the heat transferred from the turbine to the surroundings. In this way, the magnitude of the correction needed for the turbine efficiency decreased.

2.5 Engine-model tuning procedure

It is generally accepted that 1D models need a careful calibration procedure in order to obtain accurate results (Baratta et al., 2010; Gamma Technologies, 2009; Westin & Ångström, 2003), especially for turbocharged engine applications. In fact, due to their combined one-dimensional and zero-dimensional nature, these models are characterized by a simplified

description of many physical phenomena, such as: wall friction and heat transfer, concentrated losses, flow through the valves, fuel injection, and so on. Thus, they are generally not able to describe the engine fluid-dynamics accurately, unless semi-empirical input data are provided by means of the model calibration, which is usually carried out by adjusting specific model coefficients so as to accurately reproduce the experimental measurements taken at selected steady-state operating conditions.
In order to calibrate the flow losses in the intake and exhaust pipelines of a SI engine, points at wide-open throttle are more significant, due to the very high mass-flow rate. However, part-load data should also be acquired, in view of using the model for predictive purposes over a wide range of operating conditions. In general, a 1-D model will unlikely be fully predictive (i.e., quantitative) outside the calibration region, though its results may still be significant as trends. If an engine is in the early stages of design, the experimental database may be incomplete, but measurements from other engines with common or similar components may still be useful.

2.5.1 Combustion and in-cylinder heat-transfer model calibration

The accurate prediction of the in-cylinder pressure trace is mandatory for a good estimation of the engine indicated power, which in turn is fundamental to achieve the correct value of the brake power and torque. For this reason, the in-cylinder pressure is almost always acquired, on a crank angle basis, on engine test rigs. Experimental in-cylinder pressure is the main reference data for the calibration of combustion and in-cylinder heat transfer models. The x_b profile versus crank angle can be extracted by means of a diagnostic analysis (also known as heat-release analysis), (Catania et al., 2003; Guezennec & Hamada, 1999; Heywood, 1988). Then, the 'experimental' x_b profile can constitute the basis for the calibration of a predictive combustion model, can be used to set up specific lookup tables for the Wiebe parameters ('semi-predictive' approach), or it can be directly imposed in the model.
Some commercial codes, such as GT-Power, embed tools that are specifically developed for this purpose (Gamma Technologies, 2009). Using these embedded tools, most of the needed inputs for the burn rate calculation (such as trapped air-mass and residual fraction) can be worked out directly by running the simulation of the engine model. In addition, diagnostics is carried out with the same thermodynamics and chemistry as that used for the predictions. Sometimes, heat-release (HR) profiles from external diagnostic tools may be available. However, it should be pointed out that the different thermodynamic models between the diagnostic and the simulation codes can introduce additional uncertainties into the calculation of the gas thermodynamic properties as functions of temperature. For this reason, the tools provided by the adopted 1-D code for HR analysis should be used whenever possible.
As far as the calibration of the heat transfer within the cylinder is concerned, two alternatives are possible.

a. If the HR is worked out internally, the procedure allows the calibration of the heat transfer at the same time (Gamma Technologies, 2009). For example, the diagnostic tool embedded in GT-Power ('EngBurnRate' template) provides a few parameters that allow the heat-transfer calibration to be assessed. In particular, the heat transfer multiplier can be calibrated to minimize both the deviations of the so-called fuel 'lower heating value multiplier' (LHVM) from unity and the 'cumulative compression heat release'. The code

determines LHVM on the basis of an energy balance, that is similar to the one proposed in (Baratta et al., 2005; Catania et al., 2003).

b. If the heat release has been determined previously and is directly imposed, the heat transfer can only be calibrated on the basis of the match between the experimental and numerical in-cylinder pressure. However, in this case, such a calibration is also affected by an additional uncertainty, due to the calculation of the gas thermodynamic properties with different sub-models. In some applications, it may be acceptable to keep the standard C_0 coefficient, and to match the cylinder pressure by slightly shifting the HR profile. However, the alternative a) is preferable.

Once the heat transfer model has been calibrated at all the engine working points which have been investigated experimentally, the related heat-transfer multiplier values can be organized in lookup tables and then included in the engine model.

2.5.2 Turbocharged engines

The calibration procedure is more complex in the case of turbocharged engines, in which the compressor, the engine and the turbine are fluid-dynamically coupled. For turbocharged engine applications, it is not advisable to tune the entire model, consisting of the engine and the turbocharger, from the beginning. In fact, slight inaccuracies that are usually present before model tuning can make the compressor operation point (and, hence, the boost level) deviate to a great extent from the real one. In this case, it is very difficult to isolate the root cause of a performance problem (Baratta et al., 2010; Gamma Technologies, 2009; Westin & Ångström, 2003). For this reason, an engine model without the turbocharger should be built first. The intercooler outlet and the turbine inlet should be replaced by two environments in which pressure, temperature and fluid composition are properly set on the basis of measured data, and the model should be calibrated, as in the case of a naturally-aspirated engine.

2.6 Steady-state engine-model tuning example

The procedure outlined above allows the 1-D model of a turbocharged engine to obtain a rather high degree of predictability, not only in a qualitative sense, but also from a quantitative point of view. It was followed almost exactly in this way in (Baratta et al, 2010), from which Fig. 5 is taken. The engine features are reported in Table 1.

As can be seen, the engine model is generally well calibrated in all the tested cases. With reference to the whole intake system, and the portion of the exhaust ports within the cylinder head, the wall temperatures at the fluid side were set to specific values, which were selected on the basis of the outcomes of the experimental tests. The wall temperature was evaluated taking account of the gas-wall heat transfer for the pipes downstream from the exhaust ports and the external temperature was set equal to the value in the cell cabinet. The intake and exhaust ports were modelled as straight pipes, and heat-transfer multipliers were thus introduced to account for the bends, roughness, the additional surface area and turbulence caused by the valves and stems (Gamma Technologies, 2009). There was no need to set heat-transfer multipliers elsewhere in the intake system or to add friction multipliers to the model because the pressures and temperatures in the engine manifolds and ports were well reproduced (Fig. 5a,c,d). The agreement between the simulated and experimental values of PFP (peak firing pressure, Fig. 5e) and engine brake torque (Fig. 5f) demonstrate the accuracy of the combustion and engine friction sub-models, respectively. The above

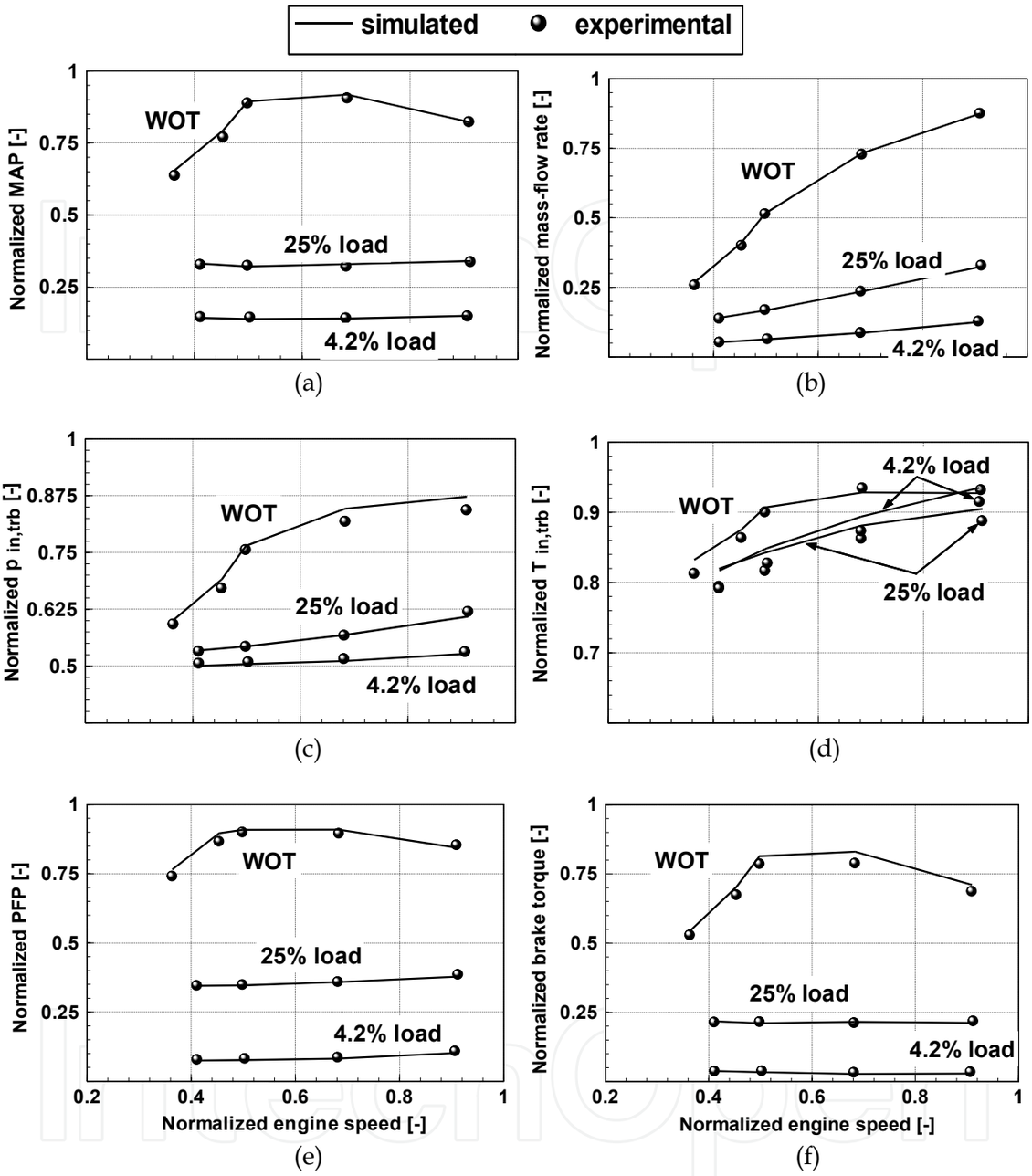

Fig. 5. Model results under steady-state working conditions, as functions of the engine speed. (a): Manifold Absolute Pressure; (b): air mass-flow rate; (c): Pressure at the turbine inlet (cylinder 1 side); (d): Temperature at the turbine inlet; (e): Peak Firing Pressure (cylinder 1); (f): Engine brake torque. Each quantity is normalized to a specific value (Baratta et al., 2010).

calibration was made with reference to the engine model without the turbocharger. Subsequently, turbocharger and intercooler (IC) were added and the pressure at the turbine outlet was tuned first, acting on the friction multipliers of the pipes located downstream from the turbine. Then, the turbine MFM and EM were adjusted so as to match both the

experimental pressure at the turbine inlet and the experimental shaft speed, and to balance the turbine and compressor cycle-averaged power:

$$\int_0^{T_{cycle}} \left[\dot{m}_{air} \cdot \frac{1}{\eta_{cmp}} \cdot c_p T^0_{in,cmp} \cdot \left(PR_{cmp}^{\gamma-1/\gamma} - 1 \right) \right] dt = \int_0^{T_{cycle}} \left[\dot{m}_{exh} \cdot \eta_{trb} \cdot c_p{}' T^0_{in,trb} \cdot \left(1 - PR^{1-\gamma'/\gamma'} \right) \right] dt \quad (11)$$

Number of cylinders	6 (in line)	Displacement	7.78 dm^3
Number of valves	4 (per cylinder)	Compression ratio	11:1
Bore	115 mm	Turbocharged	Yes
Stroke	125 mm	Intercooler	Yes

Table 1. Characteristics of a 7.8 litre turbocharged CNG engine (Baratta et al., 2010).

In particular, it is worth referring to the WOT conditions in Fig. 5, in which the first three points (engine speeds between 0.35 and 0.5 on the normalized scale) were characterized by a closed waste-gate (WG) valve, whereas the WG was partially open for the remaining two points. In those cases, the EM was selected on the basis of both the shaft speed and the pressure at the turbine inlet. MFM was selected so as to match the experimental $p_{in,trb}$ in the closed-WG points, and was then kept constant in the open-WG ones. The combined effect of MFM, EM, and WG position resulted in a slight overestimation of the turbine backpressure compared to the experiments for the open-WG points (Fig. 5c), although the differences are consistent with the uncertainty of the pressure measurements.

2.7 Transient engine simulation

The simulation of the transient behaviour of an engine by means of a 1-D simulation code is more challenging than a steady-state modelling approach. In fact, in a steady-state simulation, only the 'converged' results are significant, and the code is run until the differences in the engine variables are negligible in two consecutive simulated cycles. In a transient simulation, in which the engine speed and/or load versus time change, the model should accurately reproduce not only the engine variable at the end of the transient, but also their evolution versus time.

Engine models that have to be used for transient simulation need a more careful calibration. In particular, it is not sufficient to set the model parameters with reference to the steady-state full-load conditions. This holds for all submodels, and was demonstrated in (Lefebvre & Guilain, 2006) for the combustion model. In fact, by simulating load transients using constant full-load combustion parameters, the model results presented unacceptable deviations from the experimental ones, and did not allow transient behaviour to be predicted correctly, or different engine configurations to be compared. The model inaccuracy decreased when the combustion process was modelled as a function of the engine load and speed, and the maps were included in GT-Power, and it was further reduced when the same procedure was followed for the in-cylinder heat-transfer coefficient (c_0 in Eq. (8)). A similar procedure was followed in (Baratta et al., 2010). The following aspects should also be taken into account:

- The engine transient simulation should start from an already converged solution or, in other words, the 'actual' transient should be properly distinguished from the

'numerical' one. This can be achieved by running the model for a few seconds before the start of the 'actual' transient phase.

- The friction, filling, and heat-exchange phenomena in the intake and the exhaust manifolds should be accurately simulated. This is mandatory for turbocharged engines, in order to reproduce the experimental pressure and temperature time-history at the turbine inlet. The thermal inertia of the pipes should be taken into account in the 'actual' transient, whereas it should be neglected during the 'numerical' one, in order to shorten the thermal transient phase of the model. (Galindo et al, 2006) pointed out the great importance of the heat-transfer model in the transient calculations of a 1-D engine model. They presented a heat transfer model that is suitable to predict the transient operation of HSDI turbocharged engines when implemented in a 1-D gas-dynamic model. The model includes some selected correlations for the heat transfer coefficient for the different ducts and the engine cylinder. An important contribution of the work is the calculation of the wall temperatures by means of a three-node finite-differences scheme that accounts for thermal inertia.
- The turbine EM should be quite accurate for turbocharged engines, during the whole simulation, as it influences the slope of the boost curve versus time. Besides, it could be useful to reduce the turbocharger inertia during the 'numerical' transient. Acceptable results were obtained in (Westin & Ångström, 2003) by calibrating the turbine efficiency in the initial and in the final points of a load transient, under steady-state conditions, and by operating a linear EM interpolation during the transient evolution. In (Baratta et al., 2010), the EM was organized in a lookup table as a function of PR (see Fig. 4), and then included in the model. This led to a good model accuracy in different load-transient simulations.

Figure 6 (Baratta et al., 2010) shows the model calibration results for a tip-in event of the engine under study. The throttle was opened abruptly and the torque was varied from about 4.2% load to the steady-state values at WOT. Before applying the model to the transient simulations, the following changes were made:

- The temperature time-history for the pipes between the compressor and the intercooler was accurately simulated, taking the gas-wall heat transfer into account;
- the catalyst friction multiplier was organized in a lookup table as a function of the mass flow and was included in the model.

The model resulted to be well calibrated. In fact, not only were the asymptotic values well reproduced but also the simulated slopes that occurred during the transient were comparable to the experimental ones. However, some discrepancies were observed in the time-histories of the temperature at the turbine inlet (Fig. 6d) and the brake torque (Fig. 6f). The main differences between simulated and experimental $T_{in,trb}$ time-histories are that:

- The simulated asymptotic value at the end of the transient is higher than the experimental one. This can be ascribed to an underestimation of the measured gas temperature, which is due to the heat transferred from the thermocouple to the pipe walls by both radiation and conduction, through the thermocouple stem (Baratta et al., 2010; Westin & Ångström, 2003; Westin, 2005).
- Due to thermocouple thermal inertia, the slopes of the simulated and measured temperature rise are different. Fast temperature oscillations, such as those calculated during the first transient phase, cannot be measured by the thermocouple (Westin & Ångström, 2003).

- The computed gas temperature, before the tip-in event, is lower than that measured during the experiment. Under such a partial load, the turbocharger group produces virtually no boost, which in turn has no practical influence on the transient simulation. Therefore, the calibration of the exhaust-pipe heat-transfer multiplier and wall temperature were not performed at this operating condition, and this likely contributed to the observed difference in gas temperatures.

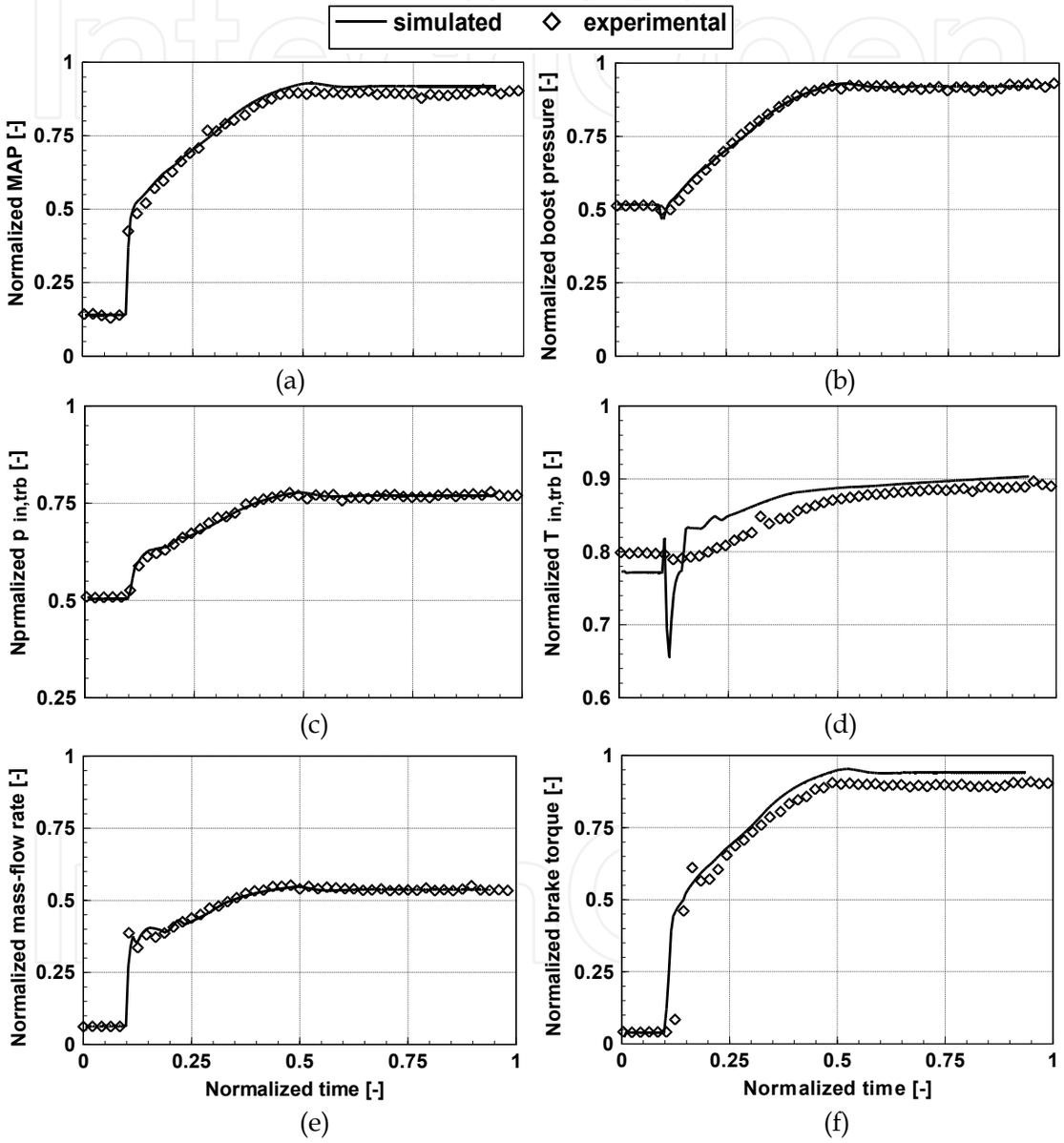

Fig. 6. Model results under transient working conditions (load step at constant engine speed, N = 0.55 N_{max}). (a) manifold absolute pressure, (b) boost pressure, (c) pressure at the turbine inlet (cylinder 1 side), (d) temperature at the turbine inlet (cylinder 1 side), (e) air mass-flow rate, (f) engine brake torque. Each quantity is normalized to a specific value (Baratta et al., 2010).

The slight difference between the calculated and the measured brake torque at the transient end (Fig. 6f) can primarily be ascribed to an underestimation of the gas pressure contribution to the friction mean effective pressure under full-load operations.
(Baratta & Spessa, 2009) modified the previous model with reference to the engine installation on a commercial vehicle for urban transportation. The model was extensively revised by modifying the pertinent pipe, bend and 'flowsplit' objects. In addition, the following differences were considered with respect to the dyno test-bed configuration:

- The bus IC was of the air-to-air type, and displayed different volumes and temperatures than the water-to-air IC installed on the dyno test rig. This influenced the engine volumetric efficiency, the charge temperature and the wave propagation phenomena within the intake system. Therefore, it was necessary to revise the IC calibration, with specific reference to flow losses and heat transfer effects (surface roughness and material, and the related multipliers).
- In the bus layout, the auxiliary components are driven by the engine, while most of them have an independent energy source or are even absent on the dyno test rig. For this reason, the engine friction-model was re-tuned in order to achieve a reliable estimation of the engine brake torque.

The new model was tuned on the basis of a specific test, in which the hydraulic torque converter of the considered urban bus was kept under stall conditions by means of the vehicle brakes, while a quick opening of the throttle valve was actuated. Throughout this transient process, the engine torque demand was thus proportional to N^2. As an example, Fig. 7 compares the experimental (black solid line) and simulated (red dotted line) time-histories of the boost pressure, mass flow rate and engine speed for a load step from $N / N_{max} = 0.3$ to 0.8. The same EM profile versus PR was used as in (Baratta et al., 2010).

3. Predictive 0-D combustion models

The reliability of the 1-D approach can be improved if predictive 0-D combustion models are used to predict the heat-release rate within the engine combustion chamber. The turbulent combustion process is a complex phenomenon that involves many chemical, thermo-dynamic and fluid-dynamic aspects, which should be studied by adopting a three-dimensional approach. However, as discussed in great detail by (Lipatnikov & Chomiak, 2002), even in this case, the development of a fundamentally substantiated model, that is, a model which is based only on the application of 'first principles', is very difficult. A possible, practical solution is that of shifting from the first principles to phenomenology, i.e., in the use of well established experimental facts and approximate descriptions of selected combustion-process characteristics which are assumed to be the main controlling factors. Similarly, predictive 0-D combustion models, which are the topic of this section, are based on a phenomenological description of the turbulent combustion process of a premixed fuel-air mixture. Although they generally need a preliminary tuning procedure, they can potentially predict the dependence of the heat-release rate on, among other factors, in-cylinder flow, combustion chamber geometry, mixture composition, thermodynamic state, and spark timing. Since the pioneering work of (Blizzard & Keck, 1974), a large number of papers have been published, which have focused on the development and/or the application of predictive combustion models to SI engines. A rather good review of the main aspects that have to be faced in a thermodynamic combustion model formulation can be found in (Velherst & Sheppard, 2009).

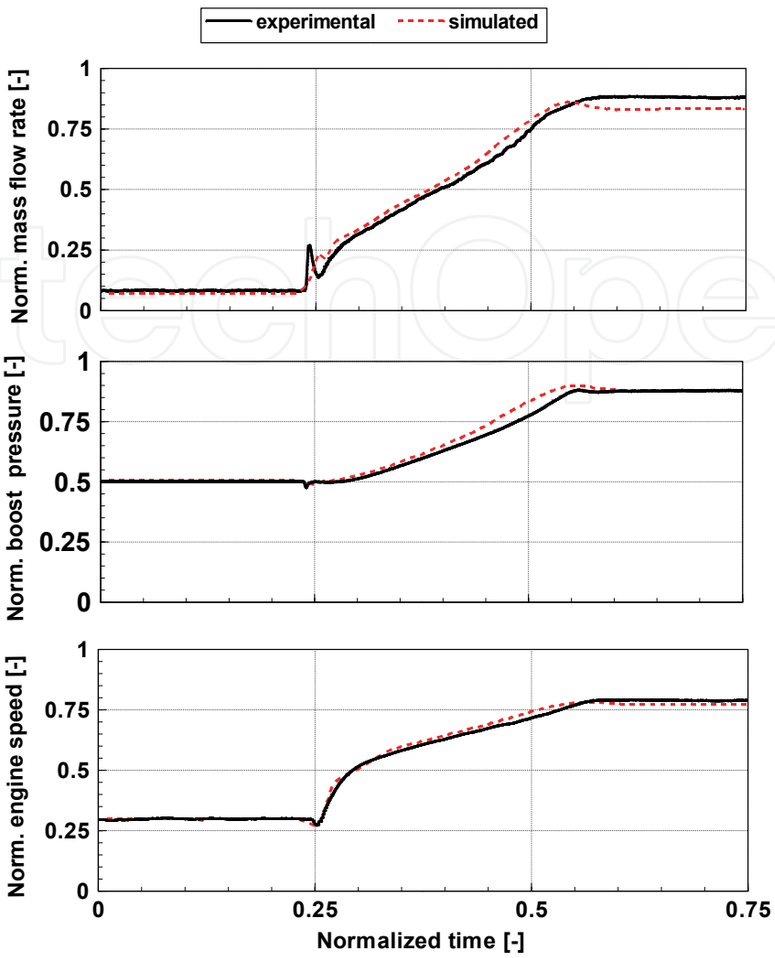

Fig. 7. Load step for an engine coupled to a stalled torque converter (Baratta & Spessa, 2009): experimental (solid black line) and simulated (red dotted line) time histories. Each quantity is normalized to a specific value.

3.1 Introduction and overview

The goal of a predictive combustion model is to predict the rate at which the unburned mixture is converted into burned gases. This allows the computation of the in-cylinder pressure through Eqs. (4-6). The different models are based on the definition of a 'turbulent burning velocity', S_b, and of a flame burning-front area A_{bf}, whereas the flame-brush thickness is generally neglected. The flame area is often modelled assuming a spherical shape of the flame front, which gradually intersects the combustion chamber surfaces as it grows (see, among others, Baratta et al., 2008; Bozza et al., 2005; Wahiduzzaman et al., 1993). This assumption has been confirmed by experiments, at least for combustion chambers with sufficiently low swirl and tumble ratios. In a thermo-dynamic modelling approach, this is also the most reasonable a priori choice. In fact, a sub-model for the flame deformation by the in-cylinder flow would need detailed information on the flow motion characteristics, which is not compatible with the thermo-dynamic nature of the overall model.

The evolution equation for the burned-gas mass fraction x_b can be derived adopting two different approaches (Baratta et al ., 2006).

a. the 'prompt burning' approach: the mixture that is entrained through the flame front burns promptly. Thus, it follows that the increment in x_b for each computational step of the combustion phase is:

$$dx_b = \frac{1}{m_{cyl}} \rho_u A_{bf} S_b \frac{d\theta}{\omega} \tag{12}$$

Examples of models based on such an approach can be found in the literature (Baratta et al., 2008; Bozza et al., 2005; D'Errico et al., 2002; Wu et al., 1993; Yoshiyama et al., 2001).

b. the 'entrainment + burning' approach: the entrainment process is followed by a laminar burnout process in the region behind the flame front. The process is described by the following equations:

$$dx_e = \frac{1}{m_{cyl}} \rho_u A_{bf} S_b \frac{d\theta}{\omega} \tag{13}$$

$$dx_b = \frac{x_e - x_b}{\tau} \tag{14}$$

x_e being the entrained mass fraction (Brown et al., 1996; Grill et al., 2006; Hattrel et al., 2006; Poulos & Heywood, 1983; Wahiduzzaman et al., 1993). The rate of laminar burnout in eq. (14) is assumed to be proportional to the unburned mass behind the flame front. Since the burnout is postulated to take place at the laminar flame speed and over a typical length scale of the turbulence microscale, the time constant τ in eq. (14) is given by the ratio of the Taylor turbulence microscale, λ, and of the laminar flame speed S_L (Wahiduzzaman et al., 1993):

$$\tau = \frac{\lambda}{S_L} \tag{15}$$

The calculation of the turbulent flame speed S_b, to be used in Eqs. (12) or (13), involves the evaluation of the laminar burning speed, S_L, of the in-cylinder turbulence generation, as well as of the turbulence-flame interaction (Baratta et al., 2006). As will be shown later on, each of these aspects can exert a remarkable influence on the indicated cycle prediction. For this reason, the assessment of the accuracy of each of the adopted sub-models is often very difficult. A comparison between simulated and experimental or diagnosed combustion-related quantities generally allows one to assess the overall simulation-model accuracy, which depends on how the different sub-model results are combined. A critical discussion of the main sub-models which are required is provided hereafter.

3.2 In-cylinder turbulence sub-model

In-cylinder turbulence modelling is required in a predictive combustion model, in order to quantify the increase in burning velocity, due to the turbulence, with respect to the case of laminar combustion. In the framework of thermo-dynamic models, a zero-dimensional model is usually applied, which provides a uniform value of the mean-flow velocity and of the root mean square (rms) turbulent fluctuation. The turbulence model results can also be

used by the in-cylinder heat-transfer sub-model, in order to derive a value for the convective heat-transfer coefficient.

A rather simple, but quite widely applied model is the K-k one (Poulos & Heywood, 1983), which is based on a zero-dimensional energy cascade from the mean flow to the viscous eddy dissipation. According to such a model, the rates of change in the mean flow kinetic energy ($K = 1/2\, m_{cyl} U^2$) and in the turbulent kinetic energy ($k = 3/2\, m_{cyl} u'^2$) are, respectively:

$$\frac{dK}{dt} = \frac{1}{2}\dot{m}_i v_i^2 - P - K\frac{\dot{m}_o}{m_{cyl}} \tag{16}$$

$$\frac{dk}{dt} = P - m_{cyl}\varepsilon - k\frac{\dot{m}_o}{m_{cyl}} \tag{17}$$

where: U is the average mean-flow velocity, u′ is the rms turbulent velocity, $\varepsilon \cong \frac{u'^3}{L_i}$ is the rate of turbulent kinetic energy dissipation per unit mass, L_i is the characteristic size of the large-scale eddies, m is the mass in the cylinder, $\dot{m}_i$ is the mass flow rate into the cylinder, $\dot{m}_o$ is the mass flow rate out of the cylinder, v_i is the jet velocity entering the chamber and P is the rate of turbulent kinetic energy production. Since the turbulence model does not spatially resolve the flow parameters, the production term P is empirically estimated from mean flow quantities:

$$P = 0.3307\, c_\beta \frac{K}{L_i}\left(\frac{k}{m}\right)^{1/2} \tag{18}$$

where the turbulent dissipation constant c_β is adjusted to give the expected profiles of u′ and U throughout the whole cycle. It is worth pointing out that the accuracy of a turbulent burning-speed model depends to a great extent on the unburned-gas turbulence evolution during combustion, which is normally thought to present a maximum near firing TDC (Baratta et al., 2008, Bozza et al, 2005, Heywood, 1988; Poulos & Heywood, 1983; Yoshiyama et al., 2001). Although the magnitude of such a maximum depends, among other factors, on the configuration of the combustion chamber and, to a lesser extent, on the intake system, its presence is generally modelled by means of heuristic approaches that add turbulence during compression and combustion. As an example, it can be seen that, in (Baratta et al., 2006, 2008; Poulos & Heywood, 1983), as soon as the combustion starts, Eq. (17) is no longer integrated, and the evolution of the turbulence intensity and of the spatial macro scale is calculated by assuming conservation of angular momentum for large scale eddies, which gives rise to an increase in the unburned-gas turbulence. Eqs. (16) and (17) have recently been modified by adding ad-hoc compression-related terms that account for the density variation in the cylinder during the compression and expansion strokes. If such terms are introduced into the K-k model equations, these also have to be integrated through the combustion phase (Bozza et al., 2005).

The main advantage of the K-k model is that of its simplicity. However, since the energy cascade is governed by the dissipation constant c_β, such a constant has to be set by the user, taking the combustion chamber geometry into account. In (Baratta et al., 2006), a sensitivity

analysis of the computed mean velocity and turbulence intensity was carried out in a range of c_β values of between 0.75 and 3.0. The experimental turbulence data close to TDC, taken in a similar motored engine to that under study, were in good agreement with the calculated levels when the value c_β=3.0 was employed.

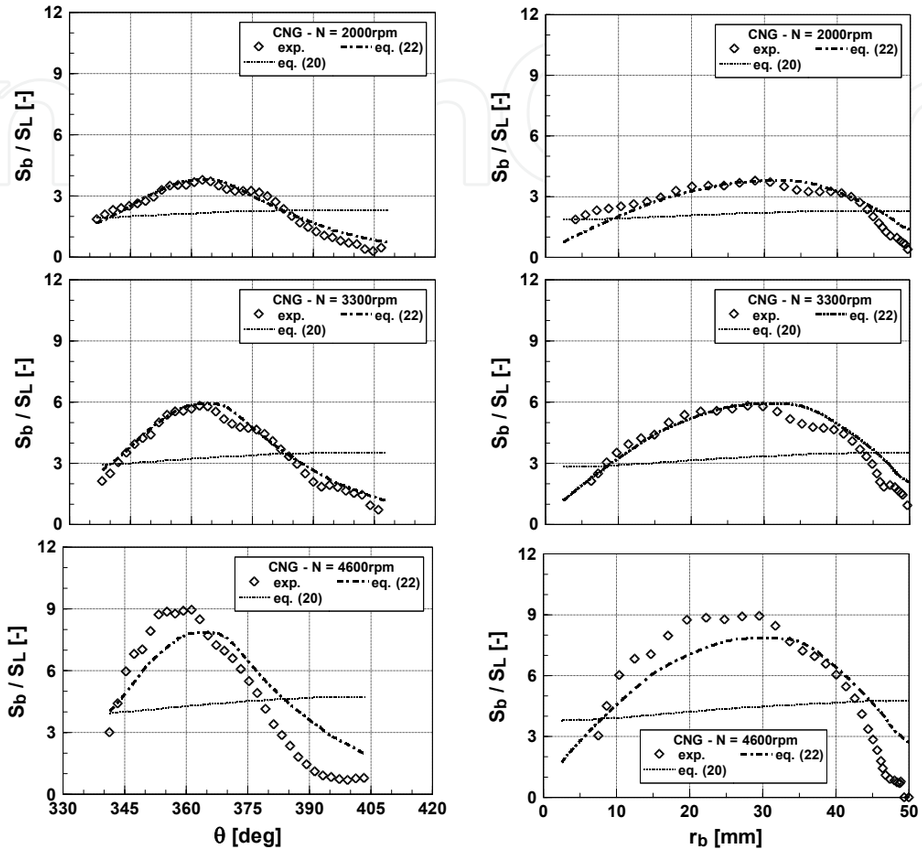

Fig. 8. Distributions of diagnosed and computed Sb/SL, versus θ (column on the left) and rb (column on the right), for different engine speeds – 2000cc 16v NA engine, CNG fuelling, bmep = 440 kPa, RAFR = 1.0, MBT timing (Baratta et al., 2006).

(Morel & Keribar, 1985) tried to develop a rather innovative flow model, with an expanded physical basis, in order to reduce the necessity of adjustments to account for engine-to-engine differences. The model was initially developed with reference to convective heat-transfer estimation in Diesel engines, and was then extended to SI engines and to the prediction of the turbulence level, for S_b prediction purposes (Morel et al., 1988). The cylinder volume is divided into multiple regions: the central core region, the squish region, the head recess region, and the piston cup region. Some axial and radial velocities are calculated, at each time step in each region, from mass conservation and piston kinematics, whereas the other radial and axial velocities, which are essentially three-dimensional, are included in the turbulence. A swirl equation, based on the conservation of angular momentum under the hypothesis of solid-body rotation, is solved for each region. The turbulent kinetic energy and the dissipation rate evolution are predicted by means of the k-ε model equations (Wilcox, 1994), which were rewritten to account for a discretization into a

few regions, rather than into a multitude of computational nodes. Thus, the turbulent kinetic energy actually includes a wide range of scales, which are partially superimposed onto the mean-flow spectrum. A turbulence production term, due to the unburned-gas compression, is also included (Morel et al., 1988). As far as the prediction of the convective heat-transfer coefficient is concerned, Morel & Keribar's model is expected to require fewer adjustments when it is applied to a new engine, due to its expanded physical basis compared to the previous models. However, when the accurate prediction of in-cylinder turbulence is required, as is the case of a predictive combustion model implementation, the proposed discretization of the k-ε model equations does not seem to be much more accurate than the very simple production term formulation given by Eq. (18). In particular, since a portion of the kinetic energy associated with the mean-flow scales is included in the turbulence terms, the simulated u' velocity may be different from the turbulent velocity which is presumed to affect the combustion velocity.

3.3 Turbulent flame-speed model

Turbulent burning-velocity models start from laminar burning speed (S_L) data for the burning mixture, and are based on the evaluation of both the turbulence level and the turbulence-flame interaction. The latter can be modelled through either a non-fractal or a fractal approach, taking the turbulence level into account. In the first approach, the entrainment velocity S_b is the sum of a convective component and a diffusive one (Wahiduzzaman et al., 1993):

$$S_b = S_L + C_s u' \left(1 - \frac{1}{1 + C_k r_b^2 / L_i^2} \right) \tag{19}$$

r_b being the burned-gas radius, L_i the turbulence macroscale and C_s and C_k two fitting parameters. The term in brackets modulates the contribution of u', in order to avoid an overprediction of the flame speed at the initial stage of combustion, when the size of the flame kernel is comparable with that of the turbulence eddies.

The second approach is based on the fractal and laminar flamelet concepts (Baratta et al., 2006; Gouldin & Miles, 1995), in order to represent the turbulent premixed flames. The laminar flamelet concept assumes that the combustion within a turbulent flame is confined to asymptotically thin moving laminar flamelets that are embedded in the turbulent flow. Since these thin layers behave like laminar flames, the turbulent burning velocity can be evaluated as the product of the surface area of the flamelets and the laminar burning speed, which is corrected to take stretch and flame curvature effects into account. The characterization and evaluation of the flamelet surface area, in relation to the turbulence properties, have been the subjects of many studies (Gülder and Smallwood, 1995; Gülder et al., 2000; North & Santavicca, 1990). According to the fractal theory, the general expression of the correlation that links the turbulent flame surface area and speed to the laminar ones is:

$$A_T / A_L = S_b / S_L = \left(\varepsilon_o / \varepsilon_i \right)^{D-2} \tag{20}$$

where A_T and A_L are the wrinkled and mean flame front surface areas, S_b and S_L represent the turbulent burning speed and the laminar flame velocity, ε_o and ε_i are the so-called outer and inner turbulence cutoff length scales, and D is the fractal dimension of the flame front

surface. The success and the applicability of these models depend to a great extent on the availability of reliable values for the inner and outer cutoff length scales and for the fractal dimension. Correlations to evaluate the cutoff length scales have been proposed, namely in (Gülder and Smallwood, 1995).

The inner cutoff length scale ε_i is taken equal to the turbulence micro scale η:

$$\varepsilon_i = \eta = L_i \left(u' L_i / \nu \right)^{-3/4} \tag{21}$$

The outer cutoff length scale has been taken equal to the integral turbulence scale, L_i, in many studies (D'Errico et al., 2002; Wu et al., 1993). However, although this choice could be acceptable for stationary flames issuing from burners (Gülder et al., 2000), in SI engine combustion, in which the mean flame front is assumed to be spherical, the wrinkling effect of turbulence on the flame front should be a function of the ratio between the characteristic flame-front and eddy dimensions, because the initially regular flame front surface progressively becomes more and more wrinkled as its dimension increases with respect to turbulent eddies. Therefore, (Baratta et al., 2006, 2008) replaced the integral length scale in Eq. (20) with a characteristic linear dimension of the flame front, i.e., the square root of its surface area. Furthermore, (Gülder et al., 2000) pointed out that, if the fractal geometry approach yields a true measure of the wrinkled surface area of the flame front, then Eq. (20) may not be a reasonable assumption for the turbulent premixed flames in the flamelet regime. In fact, small-scale turbulence can enhance the transfer of heat and species across the flame front. For this reason, (Baratta et al., 2006, 2008) introduced a pre-multiplying factor in Eq. (20), and argued that such a factor should be proportional to the average charge density, as an increased density means higher concentrations of reactive species near the flame front. Thus, the proposed formula for the turbulent burning speed was:

$$\frac{S_b}{S_L} = \left(\frac{\rho}{\rho_0} \right)^n \left(\frac{C_L \sqrt{A_{bf}}}{\eta} \right)^{D-2} = \left(\frac{\rho}{\rho_0} \right)^n \left(\frac{C_L \sqrt{A_{bf}}}{C_L \left(h_{\min} + S_p \right) \left(\frac{u' C_L \left(h_{\min} + S_p \right)}{\nu} \right)^{-3/4}} \right)^{D-2} \tag{22}$$

where h_{min} is the clearance height, S_p the instantaneous piston displacement from TDC, A_{bf} the unwrinkled flame-front area, and C_L a closure coefficient that depends on the engine fuelling and speed. n was found to be 1.25 for two different engines and ρ_0 is the average density evaluated at a reference crank angle, which depends on the specific engine (Baratta et al., 2008).

Although predictive combustion models have been developed as phenomenological models, they can simply be considered as mathematical descriptions that agree with the S-shaped mass-fraction burned observations. It is reasonable to use either Eq. (19) or the fractal approach (Eqs. (20) or (22)), coupled to the 'prompt burning' or the 'entrainment + burning' approaches, provided appropriate choices are made for A_{bf}, τ and the specific model's constants. However, though it is not a general rule, virtually all the fractal models used in the literature are coupled to the 'prompt burning' approach, whereas the non fractal ones are implemented with the 'entrainment + burning' formulation.

The results of the application of the Baratta et al. model are reported in Fig. 8, in terms of predicted S_b/S_L profiles versus crank angle and versus burned-gas radius. In the figure, 'exp.' denotes the results of the multizone diagnostic model application (Catania et al., 2004). Two calculation results are plotted: one is obtained through Eq. (22) and the other with the original Eq. (20) in which L_i is used as the outer cutoff scale. The general good agreement between the predicted and experimental results in Fig. 8 clearly shows the capability of the model to describe the flame-turbulence interaction in the overall flame propagation interval, from the development to the extinction of the flame. Furthermore, as can be inferred from this figure, Eq. (22) can extrapolate a value of S_b/S_L that is almost equal to 1 as r_b approaches zero, in agreement with the flame propagation theory (Baratta et al., 2006; Velherst & Sheppard, 2009). This supports the correctness of the introduction of the term $\sqrt{A_{bf}}$ into the definition of ε_o, as well as of the term $(\rho/\rho_0)^n$ to account for the reduced species and heat transfer across the flame front at low in-cylinder densities. If Eq. (20) is applied with $\varepsilon_o=L_i$, the modulation of S_b/S_L is insufficient, and the model generally needs special measures for a correct end-of-combustion simulation (Bozza et al., 2005; D'Errico et al., 2002; Wu et al., 1993).

The model developed in (Baratta et al., 2008) resulted to be in quite good agreement with the experimental or diagnosed combustion-related parameters. The main attractiveness of this model is given by its 'intrinsic' capability to reproduce, with good accuracy, the S_b/S_L modulation through combustion, as well as its straightforward calibration. In fact, the crank angle at which the ρ_0 term is evaluated in Eq. (22) is the only parameter that should be set for a specific engine, and it is virtually independent of fuelling and operating conditions. An example of model validation is given in the column on the left of Fig. 9: with the exception of a couple of points, the agreement of the maximum in-cylinder pressure p_{max} and the maximum heat-release rate HRR_{max} is within a few percent. Obviously, the model accuracy could be improved if an ad-hoc model tuning is carried out for each operating point, but even with a fixed calibration set for a given engine and fuelling, the degree of accuracy is acceptable, and the model can be used for predictive purposes.

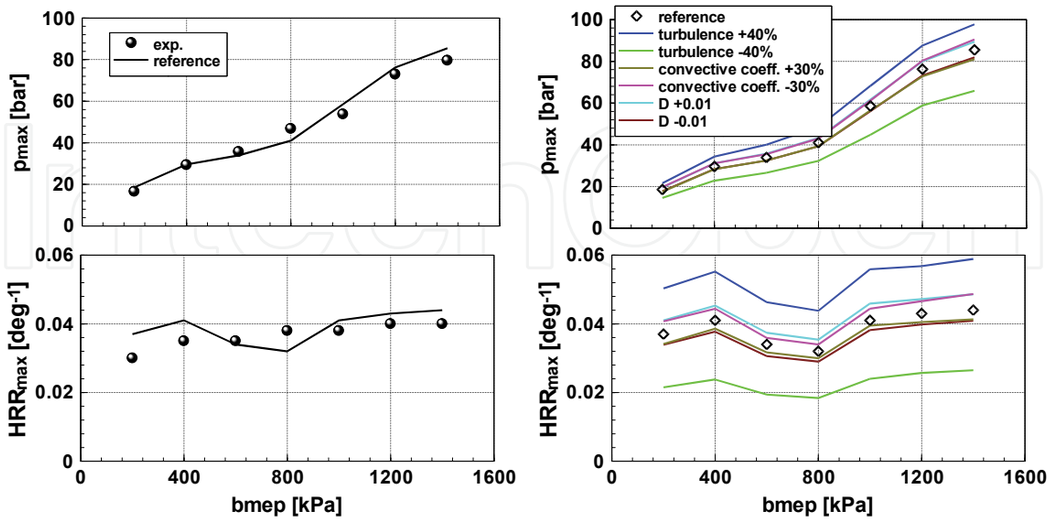

Fig. 9. Comparison between experimental/diagnosed and simulated quantities (left) and model sensitivity analysis (right) – 1200cc 8v TC engine, Methane fuelling, N = 3000 rpm, RAFR = 1.0, MBT timing.

The column on the right in Fig. 9 provides an example of the influence of the main sub-models on the results of the overall model. In-cylinder turbulence and heat-transfer sub-models are considered, and in addition, the influence of a slight change in the fractal dimension, D, is assessed. The 'reference' series is the same as in the first column, and represents the calibration in (Baratta et al., 2008). The deviation from the 'reference' calibration for each sub-model has been set on the basis of the uncertainty that can be expected in the adopted modelling framework. In particular, a deviation of 40% was considered for the turbulence level at the spark discharge, due to the significant approximations in the K-k model. An error of 30% is reasonable for the heat-transfer, especially if a diagnostic tool is not available for its calibration. Finally, the uncertainty on the fractal dimension D can be even higher than 0.01, since at present there is no agreement on its value (Baratta et al., 2006). As can be seen, for the considered deviation values, an increase in the heat-transfer coefficient has almost the same effect as a decrease in the fractal dimension. Both parameters can influence the model performance to a certain extent. As can be expected, the turbulence level exerts a remarkable influence on the overall model output. In particular, the bell-like shape of the u' profile versus crank angle, although obtained through empirical formulas, is very important to obtain an acceptable S_b/S_L profile.
The above discussion confirms that the overall model accuracy depends on each specific sub-model formulation, as well as on the related calibration. A precise model prediction can be obtained by adopting very accurate sub-models, but also when the sub-models error cancel each other. A good predictive combustion model should be formulated and calibrated so as to be able to reproduce the engine indicated cycle with a reasonable accuracy over a wide range of operating conditions, and to capture the engine performance trends when a design or operation variable is modified.

4. Conclusions

In the present chapter, the problem of the 1-D simulation the fluid-dynamics, combustion and performance of SI engines has been analyzed in detail. Among the different aspects that have to be faced when approaching this problem, the discussion has been focused on the in-cylinder pressure evolution versus crank angle, paying specific attention to the closed-valve phase, and on the turbocharger modelling. An accurate model tuning procedure has been outlined for both topics, and indications have been given on how the model could be made predictive, even in the presence of variable coefficients (such as, for example, the in-cylinder heat-transfer coefficient and the turbine efficiency multiplier).
Although quite good results can be obtained adopting of the Wiebe approach for the simulation of combustion, provided lookup tables can be built from combustion experimental data for its coefficients, the reliability of the 1-D approach can be improved to a great extent if a predictive combustion model is used for the heat-release calculations. In this case, the researcher has different options, within the fractal or non-fractal frameworks. Attention has mainly been focused on the authors' combustion model, but acceptable results can also be obtained with any model from the literature. In general, the accuracy of the overall simulation model depends on how the various sub-model results are combined.

5. References

Alkidas, A.C., "Heat Transfer Characteristics of a Spark-Ignition Engine," ASME Trans., Journal of Heat Transfer, Vol. 102, pp.189-193, 1980.

Badami, M., Millo, F., and Giaffreda, G., "Experimental and Computational Analysis of a High Performance Four-Stroke Motorcycle Engine Equipped with a Variable Geometry Exhaust System", SAE Paper 2002-01-001, 2002.

Baines, N.C., "Fundamentals of Turbocharging", Concepts NREC, White River Junction, Vermont, USA, 2005.

Baratta, M., d'Ambrosio, S., Spessa, E., and Vassallo, A., "Analysis of Cyclic Variability in a Bi-Fuel Engine By Means of a 'Cycle-Resolved' Diagnostic Technique", ASME Paper ICEF2005-1214, 2005 Fall Technical Conference of the ASME ICED, Ottawa, ON, Canada, September 11-14, 2005.

Baratta, M., Catania, A.E., Spessa, E., and Vassallo, A., "Development and Assessment of a Multizone Combustion Simulation Code for SI Engines Based on a Novel Fractal Model", SAE Paper No. 2006-01-0048, SAE 2006 World Congress, Detroit, MI, USA, April 3-6, 2006.

Baratta, M., Catania, A.E., d'Ambrosio, S., and Spessa, E., "Prediction of Combustion Parameters, Performance and Emissions in CNG and Gasoline SI Engines", ASME Transactions, Journal of Engineering for Gas Turbines and Power, Vol. 130, pp. 062805-1/11, 2008.

Baratta, M., and Spessa, E., "Turbocharged CNG Engines for Urban Transportation: Evaluation of Turbolag Reduction Strategies by means of Computational Analyses", ASME Paper No. ICES2009-76067, 2009 Spring Technical Conference of the ASME ICED, Milwaukee, Wisconsin, USA, May 3-6, 2009.

Baratta, M., Spessa, E., and Mairone, P., "Numerical Investigation of Turbolag Reduction In HD CNG Engines By Means Of Exhaust Valve Variable Actuation and Spark Timing Control", KSAE International Journal of Automotive Technology, Vol. 11 (3), pp. 289−306, 2010.

Blair, G.P., "Design and Simulation of Four Stroke Engines", SAE R-186 ISBN 0-7680-0440-3, 1999.

Blizzard, N.C., and Keck, J.C., "Experimental and Theoretical Investigation of Turbulent Burning Model for Internal Combustion Engines," SAE Paper No. 740191, 1974.

Bozza, F., Gimelli, A., Merola, S. S., and Vaglieco, B. M., "Validation of a Fractal Combustion Model Through Flame Imaging," SAE Paper No. 2005- 01-1120, 2005.

Brown, A.G., Stone, C.R., and Beckwith, P. "Cycle-by-Cycle Variations in Spark Ignition Engine Combustion – Part I: Flame Speed and Combustion Measurement and a Simplified Turbulent Combustion Model", SAE Paper No. 960612, 1996.

Catania, A.E., Misul, D., Mittica, A., and Spessa, E., "Unsteady Convection Model for Heat Release Analysis of IC Engine Pressure Data," SAE Transactions, Journal of Engines, Vol.109, pp.1610-1620, 2001.

Catania, A.E., Misul, D., Mittica, A., and Spessa, E., "A Refined Two-Zone Heat Release Model for Combustion Analysis in SI Engines," JSME International Journal, 2003, Series B, Vol. 46, No.1, pp. 75-85.

Catania, A. E., Misul, D., Spessa, E., and Vassallo, A., 2004, "A New Quasi-Dimensional Multizone Combustion Diagnostic Model for the Analysis of Heat Release, Flame

Propagation Parameters and Nitric Oxide Formation in SI Engines," Comodia '04, Yokohama, Japan, Aug. 2–5, JSME Paper No. 04-202.

D'Errico, G., Ferrari, G., Onorati, A., and Cerri, T., "Modeling the Pollutant Emissions from a S.I. Engine," SAE Paper No. 2002-01-0006, 2002.

Enomoto Y., and Furuhama, S., "A Study of the Local Heat Transfer Coefficient on the Combustion Chamber Walls of a Four-Stroke Gasoline Engine," JSME International Journal, Series II, Vol. 32, No. 1, pp.107-114, 1989.

Galindo, J., Luján, J.M., Serrano, J.R., Dolz, V., and Guilain, S., "Description of a Heat Transfer Model Suitable to Calculate Transient Processes of Turbocharged Diesel Engines With One-Dimensional Gas-Dynamic Codes", Applied Thermal Engineering, Vol.26, pp. 66–76, 2006.

Galindo, J., Luján, J.M., Serrano, J.R., Dolz, V., and Guilain, S., "Design of an Exhaust Manifold To Improve Transient Performance of a High-Speed Turbocharged Diesel Engine", Experimental Thermal and Fluid Science, Vol. 28, pp.863–875, 2004.

Gamma Technologies Inc., "GT-SUITE Engine Performance Application Manual", 2009.

Gülder, Ö.L., and Smallwood, G.J., "Inner Cutoff Scale of Flame Surface Wrinkling in Turbulent Premixed Flames," Combustion and Flame, Vol. 103, pp. 107-114, 1995.

Gülder, Ö.L., et. al., "Flame Front Surface Characteristics in Turbulent Premixed Propane/Air Combustion," Combustion and Flame, Vol. 120, pp. 407-416, 2000.

Gouldin, F.C., and Miles, P.C., "Chemical Closure and Burning Rates in Premixed Turbulent Flames", Combustion and Flame, Vol. 100, pp. 202-210, 1995.

Grill, M., Billinger, T., and Bargende, M., "Quasi-Dimensional Modeling of Spark Ignition Engine Combustion with Variable Valve Train" SAE Paper No. 2006-01-1107, SAE 2006 World Congress, Detroit, MI, USA, April 3-6, 2006.

Guezennec, Y.G., and Hamada, W., "Two-Zone Heat Release Analysis of Combustion Data and Calibration of Heat Transfer Correlation in an I.C. Engine," SAE Paper No. 1999-01-0218, 1999.

Hattrlel, T., Sheppard, C.G.W., Burluka, A.A., Neumeister, J., and Cairns, "Burn Rate Implications of Alternative Knock Reduction Strategies for Turbocharged SI Engines", SAE Paper No. 2006-01-1110, 2006.

Heywood, J.B., "Internal Combustion Engine Fundamentals," McGraw-Hill International Editions, 1988.

Hountalas, D.T., and Pariotis, E.G. "A Simplified Model for the Spatial Distribution of Temperature in a Motored DI Diesel Engine", SAE Paper no. 2001-01-1235; 2001.

Lefebvre, A., and Guilain, S., "Modelling and Measurement of the Transient Response of a Turbocharged SI Engine", SAE Paper 2005-01-0691, 2005. DOI 10.4271/2005-01-0691.

Lipatnikov, A.N., and Chomiak, J., "Turbulent Flame Speed and Thickness: Phenomenology, Evaluation, and Application in Multi-Dimensional Simulations", Progress in Energy and Combustion Science, Vol. 28, pp. 1-74, 2002.

Morel, T., and Keribar, R., "A Model for Predicting Spatially and Time Resolved Convective Heat Transfer in Bowl-in-Piston Combustion Chambers," SAE Paper 850204, 1985.

Morel, T., Rackmil, C., Keribar, R., and Jennings, M.J., "Model for Heat Transfer and Combustion in Spark Ignited Engines and its Comparison with Experiments", SAE Paper No. 880198; 1988.

North, G.L., and Santavicca, D.A., "The Fractal Nature of Premixed Turbulent Flames," Combustion Science and Technology, Vol. 72, pp. 215-232, 1990.

Onorati, A., Ferrari, G., D'Errico, G., and Montenegro, G., "The Prediction of 1D Unsteady Flows in the Exhaust System of a S.I. Engine Including Chemical Reactions in the Gas and Solid Phase", SAE Transactions, J. Engines, SAE paper 2002-01-0003; 2003.

Poulos, S.G., and Heywood, J.B., "The Effect of Chamber Geometry on Spark-Ignition Engine Combustion," SAE Paper No. 830334, 1983.

Sihling , K., and Woschni, G.: "Experimental Investigation of the Instantaneous Heat Transfer in the Cylinder of a High Speed Diesel Engine," SAE paper 790833, 1979.

Velherst, S., and Sheppard, C.G.W., "Multi-Zone Thermodynamic Modelling of Spark-Ignition Engine Combustion – An Overview", Energy Conversion and Management, Vol. 50, pp. 1326-1335, 2009.

Vítek, O., Macek, J., and Polàšek, M., "New Approach to Turbocharger Optimization using 1-D simulation tools", SAE Paper 2006-01-0438, 2006.

Wahiduzzaman, S., Morel, T., and Sheard, S., "Comparison of Measured and Predicted Combustion Characteristics of a Four-Valve SI Engine," SAE Paper No. 930613, 1993.

Watson, N., and Janota, M.S., "Turbocharging the Internal Combustion Engine", MacMillian, 1982.

Westin, F., and Ångström, H.E., "Simulation of a Turbocharged SI-Engine with Two Software and Comparison with Measured Data", SAE Paper No. 2003-01-3124, 2003.

Westin, F., Rosenqvist, J., and Ångström, H.E., "Heat Losses from the Turbine of a Turbocharged SI Engine – Measurements and Simulation", SAE Paper No. 2004-01-0996, 2004.

Westin, F., "Simulation of Turbocharged SI Engines–With Focus on the Turbine", Ph. D. Dissertation, The Royal Institute of Technology, Sweden, 2005.

Wilcox, D.C., "Turbulence Modeling for CFD", DCW Industries Inc., La Canada, California (USA), 1994.

Winkler, N., and Ångström, H.E., "Study of Measured and Model Based Generated Turbine Performance Maps within a 1D Model of a Heavy-Duty Diesel Engine Operated During Transient Conditions", SAE Paper No. 2007-01-0491, 2007.

Winterbone, D.E., and Pearson, R.J., "Design Techniques for Engine Manifolds", Professional Engineering Publishing, London, 1990.

Woschni, G., "A Universally Applicable Equation for the Instantaneous Heat Transfer Coefficient in the Internal Combustion Engine," SAE Trans., Vol. 76, pp.3065-3083, 1967.

Wu, C.M, Roberts, C.E., Matthews, R.D., and Hall, M.J., "Effects of Engine Speed on Combustion in SI Engines: Comparisons of Predictions of a Fractal Burning Model with Experimental Data", SAE Paper No. 932714, 1993.

Yoshiyama, S., Tomita, E., Zhang, Z., and Hamamoto, Y., "Measurement and Simulation of Turbulent Flame Propagation in a Spark Ignition Engine by Using Fractal Burning Model," SAE Paper No. 2001-01-3603, 2001.

Computational Simulations and Applications

Edited by Dr. Jianping Zhu

ISBN 978-953-307-430-6
Hard cover, 560 pages
Publisher InTech
Published online 26, October, 2011
Published in print edition October, 2011

The purpose of this book is to introduce researchers and graduate students to a broad range of applications of computational simulations, with a particular emphasis on those involving computational fluid dynamics (CFD) simulations. The book is divided into three parts: Part I covers some basic research topics and development in numerical algorithms for CFD simulations, including Reynolds stress transport modeling, central difference schemes for convection-diffusion equations, and flow simulations involving simple geometries such as a flat plate or a vertical channel. Part II covers a variety of important applications in which CFD simulations play a crucial role, including combustion process and automobile engine design, fluid heat exchange, airborne contaminant dispersion over buildings and atmospheric flow around a re-entry capsule, gas-solid two phase flow in long pipes, free surface flow around a ship hull, and hydrodynamic analysis of electrochemical cells. Part III covers applications of non-CFD based computational simulations, including atmospheric optical communications, climate system simulations, porous media flow, combustion, solidification, and sound field simulations for optimal acoustic effects.

How to reference

In order to correctly reference this scholarly work, feel free to copy and paste the following:

Mirko Baratta and Ezio Spessa (2011). Numerical Simulation Techniques for the Prediction of Fluid-Dynamics, Combustion and Performance in IC Engines Fuelled by CNG, Computational Simulations and Applications, Dr. Jianping Zhu (Ed.), ISBN: 978-953-307-430-6, InTech, Available from: http://www.intechopen.com/books/computational-simulations-and-applications/numerical-simulation-techniques-for-the-prediction-of-fluid-dynamics-combustion-and-performance-in-i

INTECH
open science | open minds

InTech Europe
University Campus STeP Ri
Slavka Krautzeka 83/A
51000 Rijeka, Croatia
Phone: +385 (51) 770 447
Fax: +385 (51) 686 166
www.intechopen.com

InTech China
Unit 405, Office Block, Hotel Equatorial Shanghai
No.65, Yan An Road (West), Shanghai, 200040, China
中国上海市延安西路65号上海国际贵都大饭店办公楼405单元
Phone: +86-21-62489820
Fax: +86-21-62489821

IntechOpen